Additive Manufacturing xxx (2016) xxx–xxx

Additive Manufacturing

journal homepage: www.elsevier.com/locate/addma

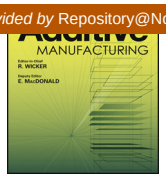

Assessing the capability of in-situ nondestructive analysis during layer based additive manufacture

Matthias Hirsch[a,b], Rikesh Patel[a], Wenqi Li[a], Guangying Guan[b], Richard K. Leach[b], Steve D. Sharples[a], Adam T. Clare[b,*]

[a] Optics and Photonics Group, Faculty of Engineering, The University of Nottingham, Nottingham NG7 2RD, United Kingdom
[b] Advanced Component Engineering Laboratory (ACEL), Faculty of Engineering, The University of Nottingham, Nottingham NG7 2RD, United Kingdom

ARTICLE INFO

Article history:
Received 2 August 2016
Received in revised form
16 September 2016
Accepted 17 October 2016
Available online xxx

Keywords:
Nondestructive evaluation
Additive manufacturing
Process control
In-situ analysis

ABSTRACT

Unlike more established subtractive or constant volume manufacturing technologies, additive manufacturing methods suffer from a lack of in-situ monitoring methodologies which can provide information relating to process performance and the formation of defects. In-process evaluation for additive manufacturing is becoming increasingly important in order to assure the integrity of parts produced in this way. This paper addresses the generic performance of inspection methods suitable for additive manufacturing. Key process and measurement parameters are explored and the impacts these have upon production rates are defined. Essential working parameters are highlighted, within which the spatial opportunity and temporal penalty for measurement allow for comparison of the suitability of different nondestructive evaluation techniques. A new method of benchmarking in-situ inspection instruments and characterising their suitability for additive manufacturing processes is presented to act as a design tool to accommodate end user requirements. Two inspection examples are presented: spatially resolved acoustic spectroscopy and optical coherence tomography for scanning selective laser melting and selective laser sintering parts, respectively. Observations made from the analyses presented show that the spatial capability arising from scanning parameters affects the temporal penalty and hence impact upon production rates. A case study, created from simulated data, has been used to outline the spatial performance of a generic nondestructive evaluation method and to show how a decrease in data capture resolution reduces the accuracy of measurement.

1. Introduction

Through the continued development of additive manufacturing (AM) processes part manufacture for high value applications is continuing to gain traction (e.g. in aerospace, medical and tooling industries) [1]. An AM process uses localised material addition on a layer per layer basis to build up three-dimensional (3D) parts [2]. Mordfin et al. define three main assumptions about manufactured materials [3]: (1) all materials contain defects; (2) these defects are expected and do not definitively mean the part is unfit for use (i.e. for service life); and (3) the detectability of defects increases with the size of the defects. These assumptions hold true for parts produced with AM processes, hence it can be deduced that inspection is essential in high value components in order to assure that the manufactured part is fit for use.

Inspection can be conducted destructively, where statistical information can be gathered in order to give a confidence interval for a part produced under similar conditions (e.g. base material consistency, temperature and atmosphere). However, for many applications in the high value added industries, destructive inspection may not be suitable (where individual part information is required). Nondestructive evaluation (NDE) of a part is, therefore, often the only method that can be employed to gather the defect data required. Everton et al. have reviewed recent research on in-situ monitoring techniques of metal AM processes [4]; an overview is given of the direct and indirect measurement instrumentation currently employed to measure parts and machine operation in AM, which has been found to be limited to a small number of commercial systems; however, there is a range of inspection techniques that are currently being developed [4] and yet there is no overarching contribution which explores their utilisation.

Measurement methods currently being considered for AM can be sorted into two principal categories: indirect and direct. Indirect measurement techniques investigate effects on part manufac-

* Corresponding author.
E-mail address: adam.clare@nottingham.ac.uk (A.T. Clare).

http://dx.doi.org/10.1016/j.addma.2016.10.004

ture based on the manufacturing environment; for example, AM machines may contain a closed-loop control for laser power in order to reduce fluctuations in the power delivery to the part being built. Contrary, direct measurement techniques assess the part based on its physical observations in order to determine quality, as a result of manufacture.

To some extent, direct measurements can be performed after the part has been produced – ex-situ (see [5–7] for recent reviews of ex-situ measurement technology applicable to AM). Ex-situ measurement allows a degree of freedom for the inspection instrument, as there are fewer space or time constraints; this is often how parts are evaluated in conventional manufacturing. However, AM provides a good opportunity for parts to be inspected as they are being built – in-situ. NDE methods that can inspect the surface and/or the subsurface region can now be used to build up an image of the internal structure of a manufactured part, ensuring it is produced to meet design parameters. In addition, measurements made and analysed in-situ can detect errors within the build process; feedback could then be used to pause the build to avoid scrappage of the flawed complete part, reducing material waste. Alternatively, the scan data can be used to enable to the AM machine to react autonomously and rework the defective layer, 'saving' the build [8]. These approaches may improve the economic viability of using AM processes and improve its adoption into more fields [9]. While the underpinning machine tool technology to allow in-situ repair is not available in current generation machines, this presents an interesting research area which will significantly enhance the capability of AM tools.

In-process monitoring is an important next step in AM methods due to user, machine and material induced errors affecting the success of manufacture from a geometrical and material point of view [4]. The study presented here investigates generic parameters of NDE tools and their influence on the productivity on the rapidly advancing AM process when incorporated in-situ. Analysing the spatial opportunity and temporal penalty associated with it, that the AM process presents for a measurement system, is a key concern when designing and selecting instruments. An NDE capability analysis approach is demonstrated in two case studies and simulated defect data is used to outline the effects of low NDE spatial capabilities.

1.1. Current inspection methods

In order to frame the methodology of determining and optimising inspection strategies, it is useful to review current measurement strategies. Indirect NDE methods currently being investigated include thermal and optical analysis – conducted either in-situ or online, have shown to yield data that can be used for feedback in selective laser melting (SLM) [10,11]. Melt pool analysis enables part failure detection. The process will infer formation of defects based on observations of the melt pool. In work by Krauss et al., artificial defects in a range of 40 μm to 500 μm were introduced into an SLM build at the design stage [12]. During part manufacture with Inconel 718 powder, the build was analysed using thermography (detecting with an infrared camera) with defects of less than 100 μm identified by detecting a variation in the cooling rate. However, as an indirect measurement method, the sizing and nature of the defects were not obtained. Doubenskaia et al. have shown that an optical system can be used for solid versus unfused powder differentiation (whilst also determining the geometry of the part in-situ) [13]. Similarly, Schwerdtfeger et al. have shown that infrared imaging, used in-situ in electron-beam powder bed fusion processes, yields layer per layer data that outlines areas of defects as a reduction in intensity [14] – in this study the minimum sampling size corresponded to 830 μm. The size range of interest for most defects in metal based AM processes is in the range of 10 μm to 100 μm [15,16].

Direct measurements investigate physical phenomena on the part in-situ. Rieder et al. have employed an ultrasonic transducer situated below the build platform to measure inconsistencies in SLM manufacture, which were tested with designed voids in the build [17]. This detection method provides limited information on the size and location of defects, providing only the layer number where a defect had been detected during the build. Research into selective laser sintering (SLS) inspected by optical coherence tomography (OCT) has shown that it is viable for in-situ process monitoring with surface and subsurface information. This was shown by Guan et al. scanning polymer test samples produced using an SLS system with embedded artificial defects [8]. Surface defects and roughness wavelengths with a minimum of 9 μm could be resolved and identification of loose powder under sintered material was possible down to 200 μm below the surface. Subsurface defects up to 100 μm in size could be identified.

Direct ex-situ part interrogation methods include the use of X-ray computed tomography (XCT) (see [7] for a thorough review), which can deliver measurements consisting of a high resolution data set of the build. For a full 3D data acquisition, Tammas-Williams et al. utilised a high resolution XCT system to scan electron-beam powder bed fusion samples with both coarse and fine scans to detect defects and relate the distribution to the processing environment [15]. The XCT analysis of electron-beam powder bed fusion samples has been shown to enable the determination of defects larger than 120 μm. Maskery et al. conducted a pore characterisation and quantification study on $AlSi_{10}Mg$ samples produced using SLM [18]. The XCT results were segmented and pores were characterised based on relative count and shape descriptors. Relative porosities of the samples were calculated to be less than 0.1% and predictions of service life were made based on the pore distributions, showing that XCT is a valid approach to SLM monitoring.

2. Defining NDE capability

Given the level of research activity in the area of NDE for AM parts, alongside the emergence of new AM machines, there is a need to evaluate how measurement techniques perform in service. The timeline of a basic in-situ analysis for an AM process is outlined in Fig. 1(a). In this case, employing an NDE method between the manufacture of a single layer will extend the time to part completion; the manufacture and measurement process need to occur in succession. Online analysis, outlined in Fig. 1(b), assumes that NDE measurements can be conducted during the manufacturing process and process measurement data on-the-fly, reducing the bottleneck apparent in the layer completion time. Full online monitoring systems can only yield indirect measurements as the solidification of the material in the manufacturing stage has to have occurred before collecting direct information.

The requirements for measurement instrumentation are dependent on the type of AM process, the materials to be used, the expected defects and the end user tolerances. This includes the spatial opportunity and temporal penalty afforded to the instrument. A definition of capability of an NDE instrument is needed in order to ascertain that it meets these requirements.

One requirement that an end user may have for production is the part completion time, $t_{manufacture}$, and is given by

$$t_{\text{manufacture}} = t_{\text{build}} + t_{\text{reset}} \quad (1)$$

where the two key time variables are the layer build stage, t_{build}, and the reset stage of each layer, t_{reset}; both expressed per layer. The layer build stage is dependent on the layer dimensions, the

Please cite this article in press as: M. Hirsch, et al., Assessing the capability of in-situ nondestructive analysis during layer based additive manufacture, Addit Manuf (2016), http://dx.doi.org/10.1016/j.addma.2016.10.004

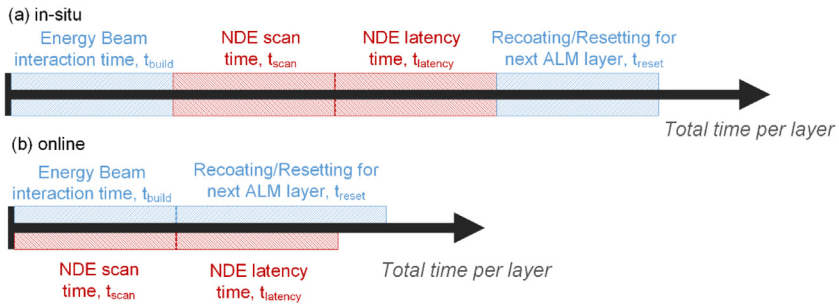

Fig. 1. (a) measurement opportunity timeline for in-situ measurement of AM processes, where all processing steps are linear and parallel processing may not be possible. (b) measurement opportunity timeline for online measurement of AM processes where some parallel processing can be done in order to optimise on NDE evaluation time in relation to AM build time.

manufacturing speed, and includes the time taken for the material to solidify from a molten state. The reset stage is the time between the layer build stage where no melting occurs, where processes such as retraction of the part in the *z*-axis, recoating with powder material (in powder bed fusion processes) or resetting to origin points for the next layer (in directed energy deposition processes) occurs.

If each layer is measured with NDE instrumentation, the overall manufacturing time ($t_{manufactureNDE}$) extends by a factor that can be defined as the temporal penalty (P_t) such that

$$t_{\mathrm{manufactureNDE}} = t_{\mathrm{manufacture}} \times \mathrm{P_t}. \quad (2)$$

Scan times of the NDE instrument are based on variables defined as scan speeds (t_{scan}) per data point, *N*, and processing/latency speeds ($t_{latency}$) per data point, *N*. For the model presented in Fig. 1(a), a sequential interaction of production and analysis is observed. The AM manufacturing with NDE time becomes

$$t_{manufactureNDE} = t_{build} + N\left(t_{scan} + t_{latency}\right) + t_{reset}. \quad (3)$$

From Eq. (3), the temporal capability can be defined, where a lower value indicates a faster scanning of the AM part in production, thus

$$P_t = N\left(t_{scan} + t_{latency}\right) / \left(t_{build} + t_{reset}\right) + 1. \quad (4)$$

The model presented in Fig. 1(b), online analysis, outlines that the scanning of the layer is occurring in parallel to manufacture. As such, scan time and latency time penalties can be disregarded and the overall temporal penalty becomes 1.

In order for the NDE instrumentation to be deemed suitable for integration into a particular AM methodology, the accuracy of the data it feeds back needs to be defined. Furthermore, there is a relationship between the scan time (temporal penalty) and the resolution of the data (e.g. pixel size) of the instrumentation that can be optimised. The importance of the resolution of data is shown in an example in Fig. 2, where a material defect is shown at its original size. The effect of resizing this image is shown to completely lose information about this defect and a description of it becomes impossible.

To quantify the resolution of the data, a spatial capability index (C_s) is defined as follows. Assuming the data acquisition of the NDE method has been optimised to yield data which is not under-sampled, the equivalent pixel size (discrimination of the instrument) is dependent on both the step size (h) and resolution (r) of the measuring instrument. The step size (h) is defined as the distance between sampled data points and the definition of resolution (r), here, is the minimum distance between two resolvable points, i.e the Rayleigh criterion. Scanning in the *xy* plane will yield the dataset of the layer but, since some processes (such as OCT, SRAS and XCT) have the ability to penetrate subsurface or near-subsurface, there is a subsurface dataset resolved in 2D (a tomograph). The step size could, hence, not be uniform in all directions and as such must be defined for each dimension separately, which would then yield distinct spatial capabilities for each dimension.

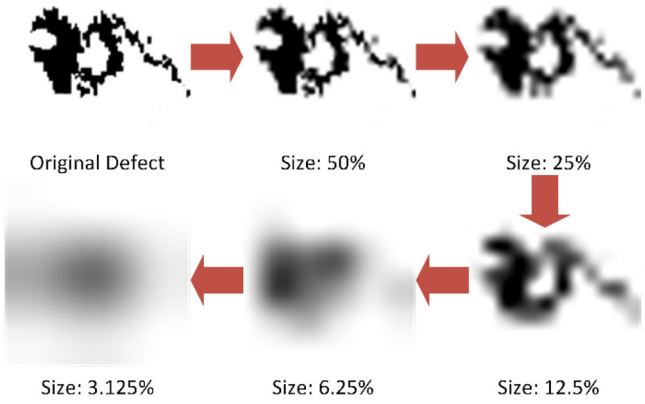

Fig. 2. An example of how resolution of the data is essential. An original defect is shown and continuously resized to show the effect of loss of data to a point where no information about the defect can be obtained.

$$h = h_X, h_Y, h_Z. \quad (5)$$

For a given process, the required spatial capability of an instrument needs to be defined by the minimum defect size, D_{min}, required to be investigated in order to determine if the part produced is fit for service, e.g. in SLM defects of approximately 10 μm are expected [15,16]. If $h_X, h_Y, h_Z < D_{\mathrm{min}}$ and the ratio of step size and resolution is adequate, then the instrument can be classed viable for use. However, generally more than one pixel is necessary for the determination of whether a defect is present or not. For this, a multiplying factor, the minimum cluster size (Clmin) needs to be defined. Combining the minimum defect size and minimum cluster size results in a capability of the NDE method to obtain data, the spatial capability: $(Cl_{min}h_X, h_Y, h_Z)/r < D_{min}$. If this spatial capability is expressed as a factor, it can be rewritten as

$$C_s = rD_{min}/Cl_{min}\left(h_X, h_Y, h_Z\right). \quad (6)$$

A minimum required spatial capability in relation to the minimum defect size is 1 at which point the NDE processing parameters will yield data with no lack of information. The outcomes of employing sub-optimal parameters (C_s below 1) are outlined in Section 4.3.

With a combination of spatial capability and temporal penalty associated to the NDE instrument, the measurement parameters and applicability of the tool for integration in AM processes can be defined. The NDE capability factors will yield empirical measures based on the processing environment of the part to be interrogated. Not only does this capability change with optimisation of the eval-

Please cite this article in press as: M. Hirsch, et al., Assessing the capability of in-situ nondestructive analysis during layer based additive manufacture, Addit Manuf (2016), http://dx.doi.org/10.1016/j.addma.2016.10.004

uation method but also with the size of the part to be produced, and must be expressed as the spatial capability and temporal penalty separately to highlight these two elements.

3. Methodology

Two case studies are presented in this work to outline how defining the NDE instrument capability can be used to present recommendations for optimisation for use on AM applications in-situ. Furthermore, a discussion on the effects of change in discrimination on the spatial capability is presented, based on simulated sets of scan data mimicking commonly observed SLM based defects.

For the first case study, an NDE technique known as spatially resolved acoustic spectroscopy (SRAS) is used to show the difference between a high resolution and low resolution scan. SRAS has been outlined as a viable candidate as an NDE method for metal-based AM [19] and can be used for the determination of surface and near subsurface feature detection. Furthermore, current research is ongoing to make SRAS applicable for obtaining surface defect and grain information on rough surfaces [20] and, hence, applicable for AM. In the past, SRAS has been employed to scan over optically smooth surfaces in order to determine microstructure and grain orientation of metals for high value applications through changes in surface acoustic wave (SAW) velocity or signal dropout. Specifically SRAS has been employed on AM samples with the intent of developing it into an in-situ investigation technology [21]. SRAS is a laser ultrasound technique that uses two separate lasers; one laser generates a SAW onto a sample projected through a defined grating, and the second laser is used to pick up the perturbation caused by the wave, enabling mapping the surface through point scans [22]. Processing data was obtained through the timestamps of data collection and set up of scan parameters. The processing time was extrapolated through timestamps of analysis data creation.

For the second case study, example scanning scenarios are shown, using optical coherence tomography (OCT) as an NDE technique for SLS of polymer powder materials. In the work by Guan et al., it was shown that OCT is capable to scan for defects and geometry features on polymer-based AM processes, both on the surface and subsurface [8]. The OCT signal is derived from back-scattering of light, hence, a higher intensity is a result of higher back scattering properties of the sample. The image depth is dependent on the penetration depth, which is determined by the properties of OCT light source and the optical properties of the target sample. The OCT case study was constructed to analyse the spatial capability and temporal penalty of two commercially available OCT systems (Zeiss Cirrus HD-OCT 5000 [23] and Topcon 3D OCT-2000 [24]).

3.1. Spatial capability on simulated defect data

A simulated data set was created to demonstrate the effects of change in instrument spatial capability. The data set was based on a typical defect array for an SLM component with defect sizes of approximately 100 μm. A sample cube of side 10 mm was defined for the creation of layer-based scan information. In order to mimic a data set that could be obtained with an NDE instrument, a 'tomograph-like' stack of images was created at a scale of 25 μm/px. These layers were defined to have a thickness of 30 μm; a common layer thickness in SLM manufacture. The data for each layer was generated with the *solid noise render function* at a random seed within an open-source software package detailed elsewhere [25]. A *pseudo-random number generator* based on current time was utilised to produce seeds in the range of 0 to $2\hat{3}1$-1, producing cloud-like variations.

For the purpose of showing the effect of a reduction in scale on spatial capability, the data set image resolution was resized in steps of 25 μm/px to 250 μm/px. The data was subsequently thresholded with a *maximum entropy function* (fixed value) [26] within ImageJ [27]. The resulting binary layer maps exhibited arbitrary groupings of dark pixels, simulating pores as defects. A full analysis could be conducted on individual stacks of grayscale images.

A statistical pore analysis, based on a pixel counting method, was then conducted on the data sets yielding absolute and relative pore area information of each layer within the set. Furthermore, an in-depth characterisation of each detectable pore was conducted. The characterisation consists of area and diameter measurements as well as two shape descriptors; the circularity and the aspect ratio of the pore. The first descriptor, f_{circ}, is defined as

$$f_{circ} = 4\pi A/P^2 \tag{7}$$

where A is the cross-sectional area and P is the perimeter length of the pore. The measure f_{circ} lies in the range $0 < f_{circ} \leq 1$, where 1 represents a perfectly circular cross-section. The second shape descriptor, f_{aspect} is defined as

$$f_{aspect} = d_{minor}/d_{major} \tag{8}$$

where the d_{minor} and d_{major} are the minimum and maximum orthogonal dimensions of the pores' best fitting ellipse. f_{aspect} can be expressed with values $0 < f_{aspect} \leq 1$, where a value of 1 indicates a perfectly spherical pore and approaching the value of 0 indicates a needle-like shape.

4. Case studies

In order to outline how the NDE capabilities can be compared for AM purposes, case studies are presented in this section. Scanning environments will be presented and discussed in relation to their applicability to AM processes as supported by the literature.

4.1. Case study 1: SRAS for SLM

SRAS has been outlined as a viable candidate for the inspection of parts produced using the SLM AM process previously [21]. A schematic of the setup of a SRAS instrument is shown in Fig. 3(a). The detected perturbation frequency indicates the SAW velocity, where the velocity contrast or wave absence can be used to obtain both the material surface microstructure and defect information. Depending on the SAW wavelength, some subsurface defect information can also be obtained. The typical SRAS scans yield data as shown in Fig. 3: the optical map (b), which directly indicates the surface cracks and pores and the velocity map (c), which images the microstructure of the sample along with defects.

The SRAS setup is a scalable system and can be customised depending on the user's requirements; there is a trade-off between accuracy and speed. In the work published, there are two sets of SRAS working parameters that are used, shown in Table 1 (with $\lambda_{saw} = 24$ μm). In the work presented by Smith et al., scans were conducted ex-situ on prepared Ti-6Al–4 V samples. In Table 1, the scan time and latency time of the instrument have been combined. The design of the instrument allows for individual selection of step size according to the movement axes utilised. The resolution is dependent on the wavelength of the SAWs. Only a single value for step size is given which indicates that $h = h_x = h_y$ with no z-axis step size present. The scans were able to gather near subsurface information – the subsurface sensitivity depth is related to the wavelength of the created SAW, approximately 24 μm.

Firstly, a coarse scan was conducted to obtain approximate surface layer information. The defined minimum defect, $D_{\min}$, was noted to be 50 μm, making it possible to determine whether large pores were present. Secondly, a fine scan was conducted, where the minimum defect size was noted to be 20 μm.

Please cite this article in press as: M. Hirsch, et al., Assessing the capability of in-situ nondestructive analysis during layer based additive manufacture, Addit Manuf (2016), http://dx.doi.org/10.1016/j.addma.2016.10.004

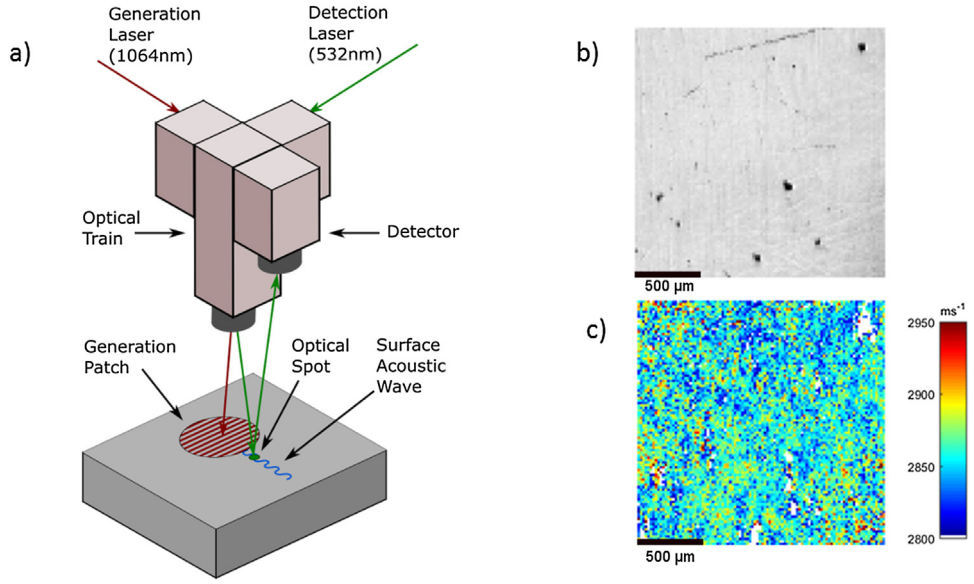

Fig. 3. (a) schematic of the SRAS system, (b) optical image and (c) acoustic image obtained from SRAS scan on AM sample from published work [21].

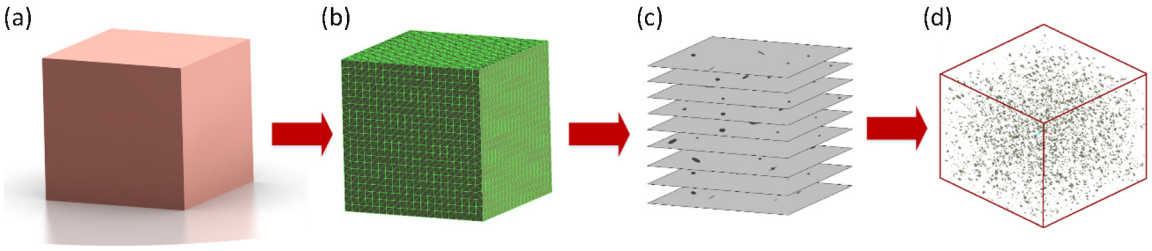

Fig. 4. Steps of manufacture with NDE instrumentation: (a) the design of the part; (b) slicing of the part to create machine code; (c) manufacture of the part on a layer per layer basis and (d) analysis also on a layer per layer basis.

Table 1
SRAS scanning parameters utilised for SLM sample measurements. After Smith et al. [21].

Example Description	Minimum Defect, D_{min} (µm)	Layer Size (µm)	Step Size, h (µm)	Resolution, r (µm)	Minimum Cluster Size, Cl_{min}	Number of data points, N	t_{scan} (s) + $t_{latency}$ (s)
SRAS coarse	50	X:10000 Y:10000	25	100	4	160000	0.0008
SRAS fine	20	X:10000 Y:10000	5	100	3	4000000	0.0008

The sample manufacturing time of the test specimen (dimensions: $10 \times 10 \times 10$ mm) was calculated to be 2072 s, arising from a hatch spacing of 75 µm, beam speed of 600 mms^{-1}, layer thickness of 30 µm and recoating time of 4 s. Using this information, the temporal penalty (per layer) for the coarse and fine scans using Eq. (4) were calculated to be 59 and 1442, respectively. Using Eq. (6), the resulting spatial capabilities are equal to 67 and 100 for the coarse and fine scan, respectively. Furthermore, data about subsurface defects is also available using SRAS – the spatial capability for subsurface information was calculated to be 69 and 21 for the coarse and fine scan, respectively.

From the presented data, it can be seen that the spatial capability of the SRAS instrument can be considered suitable for both scan environments in this requirement definition (discussed further in the simulated data case study). If the user requires a smaller D_{min}, the spatial capability would need to be changed accordingly – this in turn will affect the temporal penalty of the measuring instrument. Specifically, for SRAS integration efforts into SLM manufacture, the temporal penalty may currently be prohibitive. Therefore, further work is still required to optimise the SRAS data acquisition speed without compromising on accuracy. However, since SRAS is a scalable system, the spatial capability and its temporal penalty can be adjusted to suit the application of in-situ monitoring in AM.

4.2. Case study 2: OCT for SLS

OCT has been shown to be a viable candidate for SLS part interrogation [8]. This case study focusses on how an end user could obtain information of how capable this inspection method is, with freely available information. The two commercially available OCT systems chosen are the Cirrus HD-OCT 5000 (referred to as OCT 1) and the Topcon 3D OCT 2000 (OCT 2). Assuming a SLS test specimen was produced with dimensions of $(10 \times 10 \times 10)$ mm with a layer thickness of 100 µm, melting laser scanning speed of 2500 mms^{-1} and hatch spacing of 250 µm. The recoating mechanism takes 5 s to complete. The minimum defect size has been defined as 30 µm and the minimum cluster size has been defined as 4. The scan parameters that can be obtained from the datasheets of the OCT systems in combination with the SLS sample specimen are summarised in

Please cite this article in press as: M. Hirsch, et al., Assessing the capability of in-situ nondestructive analysis during layer based additive manufacture, Addit Manuf (2016), http://dx.doi.org/10.1016/j.addma.2016.10.004

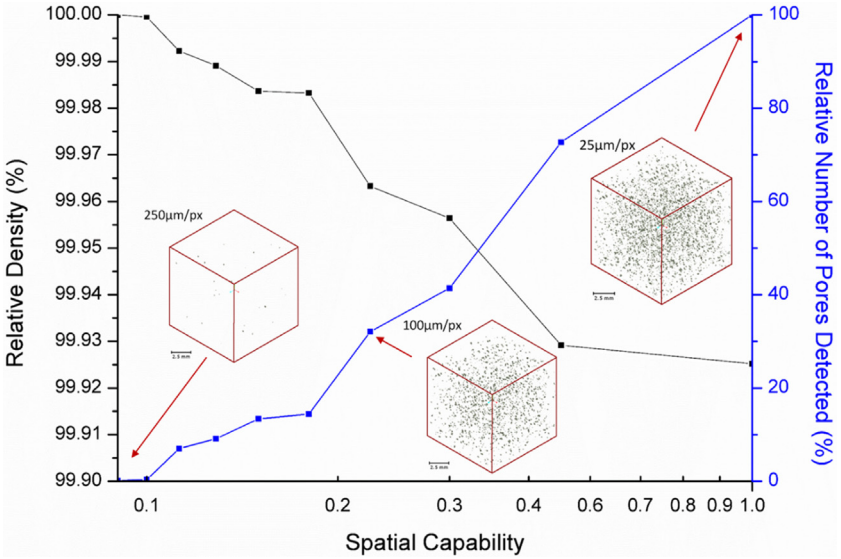

Fig. 5. Probability of Detection of defects. The number of pores detected reduces drastically with a reduction in the spatial capability of the instrument whilst the relative density of pores increases to approach 100 % density (bulk density). The insets show a 3D interpolation of the simulated scan data.

Table 2
Examples of OCT scan parameters for NDE capability calculation.

Example Description	Minimum Defect, D_{min} (µm)	Layer Size (µm)	Step Size, h (µm)	Resolution, r (µm)	Minimum Cluster Size, Cl_{min}	Number of data points, N	t_{scan} (s) + $t_{latency}$ (s)
OCT 1	30	X:10000 Y:10000	15	5	4	1332000	3.7×10^{-5}
OCT 2	30	X:10000 Y:10000	46	6	4	355550	2×10^{-5}

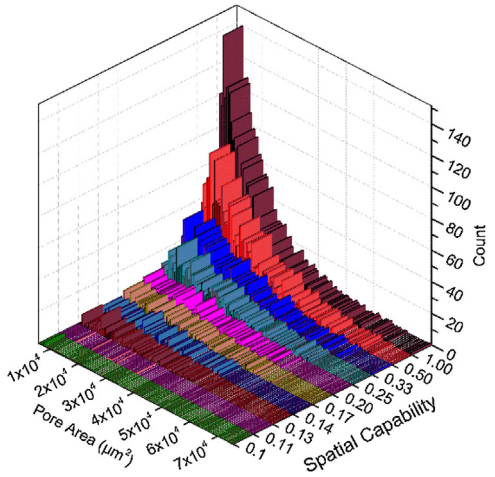

Fig. 6. Histograms representing the pore area determined by pixel counting at different spatial capabilities. The absolute number of determined pores is reduced altering the distribution.

Table 2. Only a single value for step size is given which indicates that $h = h_x = h_y$ with no z-axis step size present.

From the above presented data, both the spatial capability and temporal penalty (for $x - y$) can be calculated. In the literature, it has been outlined that OCT can return a subsurface dataset [8] but the material-specific information is not available through the data sheets. For the OCT 1 example, the temporal penalty per layer was found to be 8.5; the spatial capability was found to be 2.5. This indicates that, whilst the interrogation would considerably extend the manufacturing time of the sample cubes, the data that could be obtained from the NDE instrument would be sufficient for the requirements. In contrast, the OCT 2 example yielded a temporal penalty of 5.4 per layer and spatial capability of 0.97. The time penalty for utilising this scanning system would be lower, but the data obtained would be insufficient for the requirements stated above.

In addition, these OCT scan strategy examples help in determining the best approach for integration of OCT systems for SLS applications based on user requirements. In the case of OCT 1, the spatial capability is sufficient but efforts could be focussed on optimising the interrogation time per layer. In the case of OCT, the spatial capability could be deemed insufficient, so a redesign of the optical system could be recommended in order to meet specifications.

4.3. Simulated defect study

This section outlines the effects of non-ideal spatial capabilities of measurement instrumentation, with a focus on detectability of defects, as would be observed in AM. A statistical pore analysis is conducted on the simulated surface information that was created as described in Section 3.1. The data mimics that, which could be obtained from an AM manufacturing process such as SLM. The processing steps of such a manufacturing method are shown in Fig. 4. A common design-to-part sequence consists of the modelling of the part in CAD (Fig. 4(a)), slicing of the part to create the machine code for production (Fig. 4(b)), manufacture of the part (Fig. 4(c)), and analysis (Fig. 4(d)), where the latter two steps occur on a layer per layer basis, as is discussed previously.

Through the design of the spatial capability formula, a value between $0 < C_s < 1$ indicates a non-optimised scan environment. A C_s value of 1, by definition, shows that the NDE process is applicable for scanning, keeping in mind that the minimum defect size

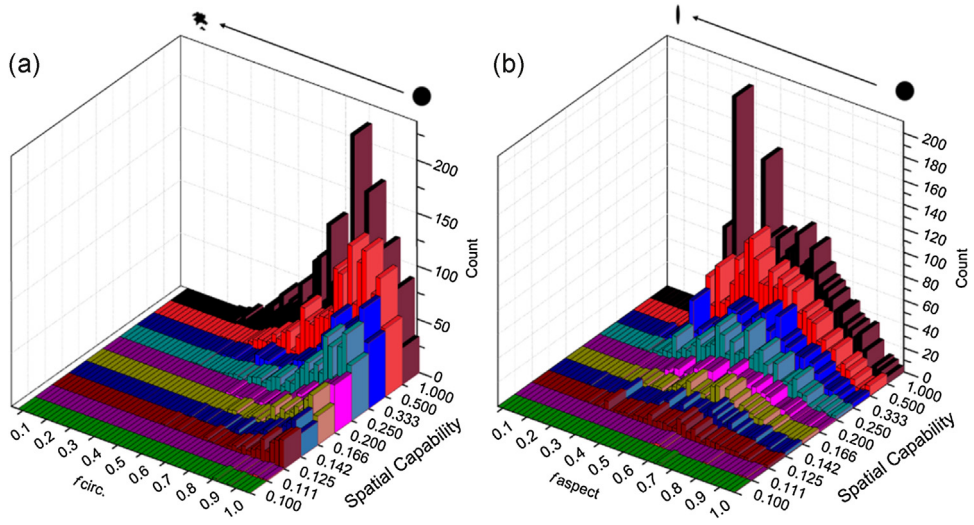

Fig. 7. Histograms of (a) circularity and (b) aspect ratio of detected pores in the simulated data sets. The shape descriptors are defined according to Eqs. (7) and (8).

has to have been set according to the microstructural requirements of the part in production. For the purposes of this study, the simulated scan data was resized to yield non-ideal spatial capability values and are compared to an ideal case scenario. The minimum defect size was defined as 100 μm and minimum cluster size is 2×2 pixels, for all discrimination changes. The relative density of pores present versus bulk material area present was calculated through pixel counting as a metric describing the relationship of apparent pores observed and a bulk density of the simulated part (100% dense in an ideal case scenario).

When the spatial capability of an NDE method is insufficient, the number of detectable defects reduces dramatically. This is shown with the probability of detection data presented in Fig. 5, where a spatial capability of 0.5 (discrimination of 50 μm/px in this case) only allows for the detection of approximately 73% of the pores present in the data set. With a further reduction in discrimination, the number of detectable pores approaches zero. This is shown with the relative part density measurement on the second ordinate in Fig. 5, where a reduction in discrimination yields a measured volumetric density approaching 100%, until no more defects are detectable. This analysis aligns with work by Maskery et al. who characterised and quantified porosity of Al-Si_{10}-Mg sample cubes produced with SLM [18]. In their study, the relative density of the test cubes, analysed with XCT, closely resembles the behaviour observed in the simulated data at a spatial capability of 1. The insets in Fig. 5, a 3D interpolation of the layer scan data, show how the decrease in spatial capability affects the available pixel data. A clear visual reduction in pores (portrayed in grey) can be observed.

In order to outline how the degrading availability of data affects measurement of defects, distribution histograms of the pore areas are shown in Fig. 6. A clear reduction in absolute number of pores detected can be observed for the reducing spatial capabilities. As soon as the data set is resized to a non-ideal capability, the distribution behaviour becomes erratic and not representative of the defects present in the simulated data. It must be mentioned that the simulated pores, similarly to real defects observed in SLM manufacture, are non-perfect spheres. This, hence, warrants the need for investigating how pore shape descriptors deviate with the alteration in discrimination.

Fig. 7 shows the circularity and the aspect ratio histograms for the simulated scan data. Trends towards a more circular pore shape (Fig. 7(a)) can be observed. Again, the absolute number of detectable pores is reflected but the results are skewed towards an f_{circ} value of 1, which is most prominent at a spatial capability of 0.2 and above. The aspect ratio, f_{aspect}, shown in Fig. 7(b) outlines a broad range with few pores perfectly round. This is also to be expected in a real scenario. With the spatial capability of the simulated data reducing, however, the random nature of the pores is not represented anymore, indicating a predictable behaviour. The shape descriptors alongside the pore area distribution are essential in defining shape geometries and it can be clearly seen that a reduction in spatial capability hinders this.

The above discussed simulated data outlines the effects when the spatial capability is below 1. Assuming the NDE instrument scan parameters have been adapted appropriately, to correlate with the minimum defect size, the capability should be a minimum of 1 to avoid loss of data. However, it must be pointed out that a spatial capability above 1 may not be ideal because it is closely linked with the scan time. It should be considered whether there is a trade-off that enables an increase in scanning time whilst not losing information.

5. Conclusions

The current drive to utilise AM technologies for high value applications is a leading factor in developing in-situ integration of NDE methods. Currently, the applicability of these processes for layer per layer scanning has not been rigorously assessed. In order to quantitatively assess the capability of a NDE method in an in-situ or online integration with an AM process, a spatial capability and temporal penalty measure need to be developed. The spatial capability describes the relationship between the minimum defect sizes, in AM production, and scan parameters that the NDE method is required to resolve accurately. Specifically, some parameters may not be uniform in all directions which is accommodated in the model. The spatial capability is defined by

$$C_s = rD_{min}/Cl_{min}\,(h_X, h_Y, h_Z)\,.$$

The temporal penalty assesses the change in time for manufacture with and without NDE instrumentation. This relationship accommodates sequential processing as well as parallel processing in that the scan latency time of the NDE process can be disregarded. In this case a time penalty of 1 is the result. Utilising the approach of measuring for temporal penalty can aid in optimising the scanning regime for allowable extra time in the AM process. The temporal penalty is defined by

$$P_t = N\left(t_{scan} + t_{latency}\right)/\left(t_{build} + t_{reset}\right) + 1.$$

Please cite this article in press as: M. Hirsch, et al., Assessing the capability of in-situ nondestructive analysis during layer based additive manufacture, Addit Manuf (2016), http://dx.doi.org/10.1016/j.addma.2016.10.004

Employing the capability measures on SRAS scans of SLM samples has shown that the system exhibits a suitable spatial capability, for both examples of coarse and fine measurement environments. However, the measurement speeds need to be enhanced for a proposed integration in SLM machines. In a further case study, it was shown how an end user could obtain information about novel NDE methods (such as OCT for SLS) and quantify the spatial capability and temporal penalty when considering for integration into AM machines. A simulated set of data was used to show how an incorrect measurement regime yields insufficient data. For a spatial capability below 1, not only the probability of detection of defects reduces drastically but also the shape descriptors used for characterising defects yield falsified data.

With utilising this NDE capability approach, optimisation of the manufacturing and interrogation environment can occur through a quantified comparative analysis.

Acknowledgements

This work was supported by "UK Research Centre in Nondestructive Evaluation" (EPSRC Grant No. EP/L022125/1), "Metrology for Precision and Additive Manufacturing" (EPSRC Grant No. EP/M008983/1) and "In-situ Monitoring of Component Integrity During Additive Manufacturing Using Optical Coherence Tomography"(EPSRC Grant No. EP/L01713X/1).

References

[1] T. Caffrey, I. Campbell, T. Wohlers, Wohlers report, in: Additive Manufacturing and 3D Printing State of the Industry, Annual Worldwide Progress Report, Wohlers Associates, Inc, Fort Collins, 2016.
[2] G.K. Lewis, E. Schlienger, Practical considerations and capabilities for laser assisted direct metal deposition, Mater. Des. 21 (4) (2000) 417–423.
[3] L. Mordfin, Nondestructive Evaluation, Materials and Processes, Part B: Processes, Marcel Dekker Inc, 1985.
[4] S.K. Everton, M. Hirsch, P. Stravroulakis, R.K. Leach, A.T. Clare, Review of in-situ process monitoring and in-situ metrology for metal additive manufacturing, Mater. Des. (2016).
[5] A. Townsend, N. Senin, L. Blunt, R.K. Leach, J.S. Taylor, Surface texture metrology for metal additive manufacturing: a review, Precis. Eng. (2016).
[6] P.I. Stavroulakis, R.K. Leach, Invited review article: review of post-process optical form metrology for industrial-grade metal additive manufactured parts, Rev. Sci. Instrum. 87 (4) (2016) 041101.
[7] A. Thompson, I. Maskery, R.K. Leach, X-ray computed tomography for additive manufacturing: a review, Meas. Sci. Technol. 27 (7) (2016) 072001.
[8] G. Guan, M. Hirsch, Z.H. Lu, D.T.D. Childs, S.J. Matcher, R. Goodridge, K.M. Groom, A.T. Clare, Evaluation of selective laser sintering processes by optical coherence tomography, Mater. Des. 88 (2015) 837–846.
[9] F. Hagemann, M. Zäh, Wirtschaftliche Fertigung Mit Rapid-Technologien: Anwender-Leitfaden Zur Auswahl Geeigneter Verfahren, Hanser, 2006.
[10] S. Clijsters, T. Craeghs, S. Buls, K. Kempen, J.P. Kruth, In situ quality control of the selective laser melting process using a high-speed, real-time melt pool monitoring system, Int. J. Adv. Manuf. Technol. 75 (5–8) (2014) 1089–1101.
[11] T. Craeghs, S. Clijsters, J.P. Kruth, F. Bechmann, M.C. Ebert, Detection of process failures in layerwise laser melting with optical process monitoring, Phys. Proc. 39 (2012) 753–759.
[12] H. Krauss, C. Eschey, M. Zaeh, Thermography for monitoring the selective laser melting process, in: Proceedings of the Solid Freeform Fabrication Symposium, Austin Texas, 2012.
[13] M. Doubenskaia, M. Pavlov, Y. Chivel, Optical system for on-line monitoring and temperature control in selective laser melting technology, Key Eng. Mater. 437 (2010) 458–461.
[14] J. Schwerdtfeger, R.F. Singer, C. Körner, In situ flaw detection by IR-imaging during electron beam melting, Rapid Prototyp. J. 18 (4) (2012) 259–263.
[15] S. Tammas-Williams, H. Zhao, F. Léonard, F. Derguti, I. Todd, P.B. Prangnell, XCT analysis of the influence of melt strategies on defect population in Ti–6Al–4éV components manufactured by Selective Electron Beam Melting, Mater. Charact. 102 (2015) 47–61.
[16] X. Zhou, D. Wang, X. Liu, D. Zhang, S. Qu, J. Ma, G. London, Z. Shen, W. Liu, 3D-imaging of selective laser melting defects in a Co–Cr–Mo alloy by synchrotron radiation micro-CT, Acta Mater. 98 (2015) 1–16.
[17] H. Rieder, A. Dillhöfer, M. Spies, J. Bamberg, T. Hess, Online monitoring of additive manufacturing processes using ultrasound, in: 11th European Conference on Non-Destructive Testing (ECNDT 2014), Prague, Czech Republic, 2014.
[18] I. Maskery, N.T. Aboulkhair, M.R. Corfield, C. Tuck, A.T. Clare, R.K. Leach, R.D. Wildman, I.A. Ashcroft, R.J.M. Hague, Quantification and characterisation of porosity in selectively laser melted Al–Si10–Mg using X-ray computed tomography, Mater. Charact. 111 (2016) 193–204.
[19] D. Clark, S.D. Sharples, D.C. Wright, Development of online inspection for additive manufacturing products, Insight Non Destruct. Test. Cond. Monit. 53 (11) (2011) 610–613, 4.
[20] S.O. Achamfuo-Yeboah, R.A. Light, S.D. Sharples, Optical detection of ultrasound from optically rough surfaces using a custom CMOS sensor, J. Phys.: Conf. Ser. 581 (2015) 012009.
[21] R.J. Smith, M. Hirsch, R. Patel, W. Li, A.T. Clare, S.D. Sharples, Spatially resolved acoustic spectroscopy for selective laser melting, J. Mater. Process. Technol. (2016).
[22] R.J. Smith, W. Li, J. Coulson, M. Clark, M.G. Somekh, S.D. Sharples, Spatially resolved acoustic spectroscopy for rapid imaging of material microstructure and grain orientation, Meas. Sci. Technol. 25 (5) (2014) 055902.
[23] Carl Zeiss Meditec AG, CIRRUS HD-OCT Advancing SMART OCT. http://www.zeiss.com/meditec/en_de/products—solutions/ophthalmology-optometry/glaucoma/diagnostics/oct/oct-optical-coherence-tomography/cirrus-hd-oct.html, (accessed 25.07.16.).
[24] Topcon Corporation, Optical Coherence Tomography 3D OCT-2000 Series. http://www.topcon-medical.eu/files/EU_Downloads/Products/3D_OCT-2000/3D_OCT_2000series_en.brochure.pdf, (accessed 25.07.16.).
[25] R.W. Solomon, Free and open source software for the manipulation of digital images, Am. J. Roentgenol. 92 (6) (2009) W330–W334.
[26] J.N. Kapur, P.K. Sahoo, A.K. Wong, A new method for gray-level picture thresholding using the entropy of the histogram, Comput. Vis. Graph. Image Process. 29 (3) (1985) 273–285.
[27] M.D. Abràmoff, P.J. Magalhães, S.J. Ram, Image processing with ImageJ, Biophoton. Int. 11 (7) (2004) 36–42.

Please cite this article in press as: M. Hirsch, et al., Assessing the capability of in-situ nondestructive analysis during layer based additive manufacture, Addit Manuf (2016), http://dx.doi.org/10.1016/j.addma.2016.10.004